Synthesis and Electrochemical Studies of a Series of Fluorinated Dodecaphenylporphyrins

Karl M. Kadish,*,† Eric Van Caemelbecke,† Francis D'Souza,† Min Lin,† Daniel J. Nurco,‡ Craig J. Medforth,*,‡ Timothy P. Forsyth,‡ Bénédicte Krattinger,‡ Kevin M. Smith,‡ Shunichi Fukuzumi,§ Ikuo Nakanishi,§ and John A. Shelnutt||

Department of Chemistry, University of Houston, Houston, Texas 77204, Department of Chemistry, University of California, Davis, California 95616, Department of Material and Life Science, Osaka University, Suita, Osaka 565-0871, Japan, Materials Theory and Computational Department, Sandia National Laboratories, Albuquerque, New Mexico 87185-1349, and Department of Chemistry, University of New Mexico, Albuquerque, New Mexico 87131

Received October 2, 1998

Dodecaphenylporphyrins with varying degrees of fluorination of the peripheral phenyl rings (F_xDPPs) were synthesized as model compounds for studying electronic effects in nonplanar porphyrins, and detailed electrochemical studies of the chloroiron(III) complexes of these compounds were undertaken. The series of porphyrins, represented as FeDPPCl and as FeF_xDPPCl where $x = 4$, 8 (two isomers), 12, 20, 28, or 36, could be reversibly oxidized by two successive one-electron transfer steps in dichloromethane to give π-cation radicals and π-dications, respectively. All of the compounds investigated could also be reduced by three electrons in benzonitrile or pyridine. In benzonitrile, three reversible reductions were observed for the unfluorinated compound FeDPPCl, whereas the FeF_xDPPCl complexes generally exhibited irreversible first and second reductions which were coupled to chemical reactions. The chemical reaction associated with the first reduction involved a loss of the chloride ion after generation of $[Fe^{II}F_xDPPCl]^-$. The second chemical reaction involved a conversion between the initially generated Fe(II) porphyrin π-anion radical and the final Fe(I) porphyrin reduction product. In pyridine, three reversible one-electron reductions were observed with the second reduction affording stable Fe(II) porphyrin π-anion radicals for all of the complexes investigated.

Introduction

Recent studies of highly substituted porphyrins (e.g., **1**−**4** in Figure 1) have revealed many structural, spectroscopic, and chemical changes associated with the substituent-induced nonplanarity present in such systems[1−15] and have raised the question of whether nonplanar distortions may have a functional role in the energetics of biological systems.[16] The substituents in highly substituted porphyrins exert a complex mixture of steric effects (which dictate the amount and type of nonplanar distortion) and electronic effects (resulting from the electron-donating or electron-withdrawing abilities of the substituents) which can lead to some quite unexpected behavior. For example, progressive brominations of **5** (to ultimately yield **6**) initially produce the expected increase in half-wave potential for oxidation of the porphyrin, but then begin to decrease the oxidation potential as the degree of macrocyclic nonplanarity increases significantly for the more highly brominated analogues.[17−20] One aim of our research is to study the steric and electronic effects of substituents in nonplanar porphyrins and to obtain spectroscopic data which might be used to differentiate these effects in biologically important systems. To this end, we recently reported studies of a series of nickel(II) tetraalkylporphyrins (**7**−**10**) where the steric bulk of the peripheral substit-

† University of Houston.
‡ University of California.
§ Osaka University.
|| Sandia National Laboratories and University of New Mexico.

(1) Barkigia, K. M.; Berber, M. D.; Fajer, J.; Medforth, C. J.; Renner, M. W.; Smith, K. M. *J. Am. Chem. Soc.* **1990**, *112*, 8851.
(2) Barkigia, K. M.; Chantranupong, L.; Smith, K. M.; Fajer, J. *J. Am. Chem. Soc.* **1988**, *110*, 7566.
(3) Renner, M. W.; Barkigia, K. M.; Zhang, Y.; Medforth, C. J.; Smith, K. M.; Fajer, J. *J. Am. Chem. Soc.* **1994**, *116*, 8582.
(4) Sparks, L. D.; Medforth, C. J.; Park, M.-S.; Chamberlain, J. R.; Ondrias, M. R.; Senge, M. O.; Smith, K. M.; Shelnutt, J. A. *J. Am. Chem. Soc.* **1993**, *115*, 581.
(5) Barkigia, K. M.; Nurco, D. J.; Renner, M. W.; Melamed, D.; Smith, K. M.; Fajer, J. *J. Phys. Chem. B* **1998**, *102*, 322.
(6) Drain, C. M.; Kirmaier, C.; Medforth, C. J.; Nurco, D. J.; Smith, K. M.; Holten, D. *J. Phys. Chem.* **1996**, *100*, 11984.
(7) Gentemann, S.; Nelson, N. Y.; Jaquinod, L.; Nurco, D. J.; Leung, S. H.; Medforth, C. J.; Smith, K. M.; Fajer, J.; Holten, D. *J. Phys. Chem. B* **1997**, *101*, 1247.
(8) Medforth, C. J.; Smith, K. M. *Tetrahedron Lett.* **1990**, *31*, 5583.
(9) Nurco, D. J.; Medforth, C. J.; Forsyth, T. P.; Olmstead, M. M.; Smith, K. M. *J. Am. Chem. Soc.* **1996**, *118*, 10918.
(10) Hobbs, J. D.; Majumder, S. A.; Luo, L.; Sickelsmith, G. A.; Quirke, J. M. E.; Medforth, C. J.; Smith, K. M.; Shelnutt, J. A. *J. Am. Chem. Soc.* **1994**, *116*, 3261.
(11) Senge, M. O.; Smith, K. M. *J. Chem. Soc., Chem. Commun.* **1994**, 923.
(12) Bhyrappa, P.; Krishnan, V. *Inorg. Chem.* **1991**, *30*, 239.
(13) Bhyrappa, P.; Krishnan, V.; Nethaji, M. *J. Chem Soc., Dalton Trans.* **1993**, 1901.
(14) Bhyrappa, P.; Krishnan, V.; Nethaji, M. *Chem. Lett.* **1993**, 869.
(15) Wijesekera, T.; Matsumoto, A.; Dolphin, D.; Lexa, D. *Angew. Chem., Int. Ed. Engl.* **1990**, *29*, 1028.
(16) Shelnutt, J. A.; Song, X.-Z.; Ma, J.-G.; Jai, S.-L.; Jentzen, W.; Medforth, C. J. *Chem. Soc. Rev.* **1998**, *27*, 31.
(17) D'Souza, F.; Villard, A.; Caemelbecke, E. V.; Franzen, M.; Boschi, R.; Tagiagtesta, P.; Kadish, K. M. *Inorg. Chem.* **1993**, *32*, 4042.
(18) Kadish, K.; D'Souza, F.; Villard, A.; Autret, M.; Van Caemelbecke, E.; Bianco, P.; Antonini, A.; Tagliatesta, P. *Inorg. Chem.* **1994**, *33*, 5169.
(19) Tagliatesta, P.; Li, J.; Autret, M.; Van Caemelbecke, E.; Villard, A.; D'Souza, F.; Kadish, K. *Inorg. Chem.* **1996**, *35*, 5570.
(20) Kadish, K. M.; Li, J.; Van Caemelbecke, E.; Ou, Z.; Guo, N.; Autret, M.; D'Souza, F.; Tagliatesta, P. *Inorg. Chem.* **1997**, *36*, 6292.

10.1021/ic9811695 CCC: $18.00
Published on Web 04/14/1999

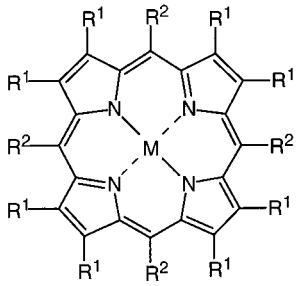

	R^1	R^2	M	Abbreviation
1	ethyl	phenyl	2H	
2	ethyl	NO_2	2H	
3	Br	phenyl	2H	
4	phenyl	phenyl	2H	
5	H	phenyl	$Fe^{III}Cl/Co^{II}$	
6	Br	phenyl	$Fe^{III}Cl/Co^{II}$	
7	H	methyl	Ni^{II}	
8	H	ethyl	Ni^{II}	
9	H	i-propyl	Ni^{II}	
10	H	t-butyl	Ni^{II}	
11	phenyl	4-fluorophenyl	2H	H_2F_4DPP
12	4-fluorophenyl	phenyl	2H	H_2F_8DPP (β)
13	phenyl	2,6-difluorophenyl	2H	H_2F_8DPP (meso)
14	4-fluorophenyl	4-fluorophenyl	2H	$H_2F_{12}DPP$
15	phenyl	pentafluorophenyl	2H	$H_2F_{20}DPP$
16	4-fluorophenyl	pentafluorophenyl	2H	$H_2F_{28}DPP$
17	3,5-difluorophenyl	pentafluorophenyl	2H	$H_2F_{36}DPP$
18	2,6-difluorophenyl	pentafluorophenyl	2H	$H_2F_{36}DPP$
19	pentafluorophenyl	pentafluorophenyl	2H	$H_2F_{60}DPP$
20	2,6-difluorophenyl	phenyl	2H	$H_2F_{16}DPP$
21	pentafluorophenyl	phenyl	2H	$H_2F_{40}DPP$

Figure 1. Structures of the porphyrins discussed in this work.

uents was used to vary the degree of porphyrin nonplanarity while the electronic properties of the substituents were held relatively constant.[21] In the work presented here, a series of porphyrins are described for which the converse should be true, namely, that electronic effects should predominate because the steric effects of the substituents, as demonstrated by molecular modeling studies,[22] are reasonably constant.

The series of porphyrins synthesized are based on the dodecaphenylporphyrin (DPP) framework (**4**) and have a total of 4, 8 (two isomers), 12, 20, 28, or 36 fluorines on the peripheral phenyl rings (**11**−**17**). The fluorinated DPPs (F_xDPPs) were chosen for this work because they offered the greatest potential for varying electronic effects while at the same time minimizing differences in the steric effects of the substituents, and because existing synthetic methodology could be applied to the preparation of these materials. An investigation of the electrochemical properties of the chloroiron(III) complexes of DPP and the F_xDPPs (abbreviated as FeDPPCl and FeF_xDPPCls) confirms the dominance of electronic changes in the series; oxidation of the macrocycle (in CH_2Cl_2) becomes more difficult and reduction of the macrocycle or iron atom (in benzonitrile or pyridine) more facile as the degree of fluorination is increased. In addition, the electrochemical studies reveal that the site of the second reduction is strongly dependent on the macrocycle substituents and on the solvent. For the FeF_xDPPCl complexes in benzonitrile a novel intramolecular electron transfer between an initially generated Fe(II) porphyrin π-anion radical and a final Fe(I) porphyrin species is observed.

Experimental Section

Spectroscopy. ^{1}H and ^{19}F NMR spectra were measured at frequencies of 300 and 283 MHz, respectively. Spectra were typically recorded at ambient temperature (298 ± 5 K) using 2−5 mM solutions in $CDCl_3$. ^{1}H chemical shifts were referenced to the chloroform solvent peak at δ 7.26. ^{19}F chemical shifts were referenced to CF_2Cl_2 at −8.0 ppm.[23] Visible absorption spectra were recorded on a Hewlett-Packard 8450A spectrophotometer using CH_2Cl_2 as solvent. High-resolution FAB or EI mass spectra were obtained from the UC Riverside facility. Low-resolution MALDI spectra were obtained at UC Davis as described previously.[24]

Electrochemistry. Benzonitrile was distilled over P_2O_5 under vacuum, and pyridine was distilled over CaH_2 prior to use. Tetra-*n*-butylammonium perchlorate (TBAP) was recrystallized from ethyl alcohol and dried in a vacuum oven at 40 °C for at least 1 week prior to use. Cyclic voltammetry was carried out using an EG&G Model 173 potentiostat coupled with an EG&G Model 175 universal programmer or a BAS 100 electrochemical analyzer. Current−voltage curves were recorded on an EG&G Princeton Applied Research Model RE-0151 XY recorder. A three-electrode system was used and consisted of a glassy carbon working electrode, a platinum wire counter electrode, and a saturated calomel reference electrode (SCE). The reference electrode was separated from the bulk solution by a fritted-glass bridge filled with the solvent/supporting electrolyte mixture. Ferrocene was used as the internal standard, but all potentials were referenced to the SCE. Solutions containing the metalloporphyrins were deoxygenated by a stream of nitrogen for at least 5 min prior to running the

(21) Jentzen, W.; Hobbs, J. D.; Simpson, M. C.; Taylor, K. K.; Ema, T.; Nelson, N. Y.; Medforth, C. J.; Smith, K. M.; Veyrat, M.; Mazzanti, M.; Ramasseul, R.; Marchon, J.-C.; Takeuchi, T.; Goddard, I., W. A.; Shelnutt, J. A. *J. Am. Chem. Soc.* **1995**, *117*, 11085.

(22) Muzzi, C. M.; Medforth, C. J.; Nurco, D. J.; Clement, T. E.; Khoury, R. G.; Smith, K. M.; Cancilla, M.; Voss, L.; Lebrilla, C.; Ma, J.-G.; Shelnutt, J. A. Manuscript in preparation.

(23) Harris, R. K.; Mann, B. E. *NMR and the Periodic Table*; Academic Press: New York, 1978; p 99.

(24) Green, M. K.; Medforth, C. J.; Muzzi, C. M.; Nurco, D. J.; Shea, K. M.; Smith, K. M.; Shelnutt, J. A.; Lebrilla, C. B. *Eur. Mass Spectrosc.*, **1997**, *3*, 439.

experiments and were also protected from air by a nitrogen blanket during the experiment. Thin-layer spectroelectrochemical measurements were carried out with a Tracor Northern 6500 multichannel analyzer/controller coupled with an EG&G Model 173 universal programmer using an optically transparent platinum thin-layer working electrode.[25] ESR spectra of the doubly reduced FeF_{20}DPPCl generated electrochemically were taken on a JEOL JES-RE1XE by using an electrolysis cell designed for ESR measurements.[26] The controlled-potential electrolysis of FeF_{20}DPPCl was carried out in benzonitrile containing 0.2 M TBAP in the ESR cavity.

Syntheses of Pyrroles and Precursors. 3,4-Bis(4-fluorophenyl)-pyrrole. The title compound was prepared by adapting a procedure used to prepare 3,4-diphenylpyrrole.[27] A 2 L three-necked round-bottomed flask was filled with anhydrous MeOH (1400 mL), NaOMe (211.7 g, 3.9 mol), and dimethyl *N*-acetyliminodiacetate[28] (79.6 g, 0.39 mol) and brought to a gentle reflux under an inert atmosphere. 4,4′-Difluorobenzil (96.4 g, 0.39 mol, Aldrich) was added, and the solution was refluxed for an additional 25 min, after which the reaction contents were poured into deionized H_2O (6 L). A precipitate formed and was filtered off, and the aqueous filtrate was washed with diethyl ether (2 × 1 L). The residual diethyl ether and MeOH present in the aqueous solution were removed by partially stripping off the solvent in vacuo. The cooled concentrated aqueous solution was acidified with 6 M HCl, resulting in the precipitation of a mix of diester and partially hydrolyzed diester diphenylpyrroles (34.2 g), which was filtered off.

To afford a complete saponification, the crude diester diphenylpyrroles (32.3 g) were dissolved in 10% aqueous KOH (350 mL) and refluxed for 20 min. The stirred solution was chilled in an ice bath and neutralized by the addition of 6 M HCl, which precipitated the diacid pyrroles. Filtration of the precipitate afforded a mixture of 3,4-bis(4-fluorophenyl)pyrrole-2,5-dicarboxylic acid, 3,4-bis(4-methoxyphenyl)-pyrrole-2,5-dicarboxylic acid, and 3-(4-fluorophenyl)-4-(4-methoxyphenyl)pyrrole-2,5-dicarboxylic acid as a brittle tan solid (32.1 g). The formation of methoxylated pyrroles presumably takes place via nucleophilic substitution of the aryl fluorines by methoxide.

The diacid diphenylpyrrole mixture (32.1 g) was dissolved in ethanolamine (200 mL) and refluxed for 2 h. The cooled reaction solution was poured into a mixture of H_2O (1 L) and saturated aqueous NaCl (500 mL), and the aqueous phase was extracted with CH_2Cl_2 (3 × 300 mL). The pooled organic extracts were dried over anhydrous Na_2SO_4 and stripped of solvent in vacuo to yield a dark brown residue. The residue was chromatographed on silica gel eluted with gradient mixtures of CH_2Cl_2/petroleum ether. After several columns and crystallizations from CH_2Cl_2/cyclohexane, three diphenylpyrroles were isolated in pure form. The least polar fractions afforded 3,4-bis(4-fluorophenyl)pyrrole (6.8 g, 0.027 mol, 6.9% yield based on starting 4,4′-difluorobenzil), while the most polar fractions afforded 3,4-bis-(4-methoxyphenyl)pyrrole (4.5 g, 0.016 mol) in 4.1% yield. Of intermediate R_f on silica gel was 3-(4-fluorophenyl)-4-(4-methoxyphenyl)pyrrole (3.5 g, 0.013 mol), which was isolated in 3.3% yield. Characterization data for these compounds are as follows.

3,4-Bis(4-fluorophenyl)pyrrole. ^{1}H NMR ($CDCl_3$): δ 8.29 (br s, 1H, NH), 7.19 (m, 4H, H_{ortho}), 6.95 (m, 4H, H_{meta}), 6.78 (d, J = 2.7 Hz, 2H, pyrrole-H_α). ^{13}C NMR ($CDCl_3$): δ 115.06 (d, J = 21.2 Hz, C_{meta}), 117.23 (s, C_α), 122.52 (s, C_β), 129.93 (d, J = 7.7 Hz, C_{ortho}), 131.50 (d, J = 2.7 Hz, C_{ipso}), 161.39 (d, J = 244.3 Hz, C_{para}). ^{19}F NMR ($CDCl_3$): δ −119.2 (m, F_{para}). Mp: 138−140 °C. EI$^+$ HRMS: calcd 255.0860, found 255.0865 (M^+ 100). Anal. Calcd for $C_{16}H_{11}F_2N$: C 75.28, H 4.34, N 5.49. Found: C 75.30, H 4.37, N 5.51. Alternate preparation: European Patent 0 334 147.

3,4-Bis(4-methoxyphenyl)pyrrole. ^{1}H NMR ($CDCl_3$): δ 8.20 (br s, 1H, NH), 7.18, 6.81 (d, 4H each, H_{ortho}, H_{meta}, J = 8.9 Hz), 6.79 (d, 2H, H_α), 3.76 (s, 6H, −OCH_3). ^{13}C NMR ($CDCl_3$): δ 55.14 (−OCH_3), 113.62 (C_{meta}), 116.75 (C_α), 122.96 (C_β), 128.42 (C_{ipso}), 129.53 (C_{ortho}), 157.76 (C_{para}). Mp: 110.5−112.5 °C. EI$^+$ HRMS: calcd 279.1259, found 279.1251 (M^+ 100). Anal. Calcd for $C_{18}H_{17}NO_2$: C 77.40, H 6.13, N 5.01. Found: C 77.71, H 6.18, N 5.10.

3-(4-Fluorophenyl)-4-(4-methoxyphenyl)pyrrole: isolated as an oil or glasslike material. EI$^+$ HRMS: calcd 267.1059, found 267.1057 (M^+ 100).

3,4-Bis(3,5-difluorophenyl)pyrrole. 3,5,3′,5′-Tetrafluorobenzil was prepared by adapting a standard procedure for the condensation of benzaldehyde into benzoin[29] followed by an oxidation to the corresponding benzil.[30] Thiamine hydrochloride (11.0 g, 0.033 mol) was dissolved in deionized H_2O (32 mL), followed by the addition of 95% ethanol (85 mL), 10% sodium hydroxide (32 mL), and 3,5-difluorobenzaldehyde (45.0 g, 0.317 mol, Indofine Chem. Co.). The mixture was stoppered, shaken vigorously, and allowed to sit for 3 days. The solution was then filtered and the filtrate washed with deionized H_2O and vacuum-dried to afford 3,5,3′,5′-tetrafluorobenzoin (36 g, 0.13 mol).

3,5,3′,5′-Tetrafluorobenzoin (36 g, 0.13 mol) and aqueous acidic cupric acetate (16 mL of 10% acetic acid containing 0.48 g of cupric acetate dihydrate) were then dissolved in a solution of ammonium nitrate (12.7 g, 0.158 mol) in glacial acetic acid (80 mL). The reaction mixture was refluxed for 90 min, cooled, and filtered, and the filtrate was washed with deionized H_2O. The crude product was recrystallized from MeOH to afford 3,5,3′,5′-tetrafluorobenzil (28.0 g, 0.099 mol) in 62% yield (based on starting 3,5-difluorobenzaldehyde). ^{1}H NMR ($CDCl_3$): δ 7.5 (m, 4H, H_{ortho}), 7.1 (m, 2H, H_{para}). ^{19}F NMR ($CDCl_3$): δ −108.0 (m, F_{meta}). Mp: 135.0−136.5 °C. EI$^+$ HRMS: *m*/*z* for $C_{14}H_6F_4O_2$ M^+ (not found); however, a fragment (found: 141.0136) corresponds to $C_7H_3F_2O$ (calcd: 141.0151), presumably resulting from cleavage of the C−C bond. Anal. Calcd for $C_{14}H_6F_4O_2$: C 59.59, H 2.14. Found: C 59.66, H 2.11.

3,4-Bis(3,5-difluorophenyl)pyrrole was prepared by adapting the procedure used to prepare 3,4-diphenylpyrrole.[27] A 2 L three-necked round-bottomed flask was filled with anhydrous MeOH (600 mL), NaOMe (65.0 g, 1.20 mol), and dimethyl *N*-acetyliminodiacetate (110.4 g, 0.544 mol), and the solution was refluxed for 15 min under an inert atmosphere. The reflux was temporarily stopped to allow the addition of 3,5,3′,5′-tetrafluorobenzil (75.0 g, 0.266 mol), after which the solution was refluxed for an additional 40 min and poured into deionized H_2O (6 L). In some cases, a precipitate was observed when the reaction mixture was poured into deionized H_2O, and this was most evident when the reaction was carried out on a smaller scale. The precipitate was a reaction byproduct resulting from the benzil−benzilic acid rearrangement[31] of 3,5,3′,5′-tetrafluorobenzil and was filtered off. The aqueous solution was washed with diethyl ether (2 × 2 L), and the residual diethyl ether and MeOH present in the aqueous solution were removed under vacuum. The cooled concentrated aqueous solution was basified by the addition of NaOH (600 g) and boiled in two 4 L beakers for 30 min. The solutions were allowed to cool for 6 h, placed in ice baths, and acidified by the dropwise addition of 6 M HCl to precipitate the diacid pyrrole. The precipitate was filtered off and dried in vacuo, yielding 3,4-bis(3,5-difluorophenylpyrrole)-2,5-dicarboxylic acid as a tan solid (16.7 g; EI$^+$ HRMS: calcd 379.04677, found 379.04662).

3,4-Bis(3,5-difluorophenylpyrrole)-2,5-dicarboxylic acid (16.7 g) was dissolved in ethanolamine (250 mL) and refluxed for 2 h. The cooled solution was poured into a mixture of deionized H_2O (500 mL) and saturated aqueous NaCl (250 mL) and extracted with CH_2Cl_2 (3 × 150 mL). The combined organic extracts were washed with a mixture of deionized H_2O (500 mL) and saturated aqueous NaCl (250 mL), dried over anhydrous Na_2SO_4, and stripped of solvent in vacuo to afford a thick brown oil. This oil solidified upon storage at −60 °C and also remained a solid when warmed to room temperature. This material was chromatographed on a silica gel column eluted with CH_2Cl_2 to afford 3,4-bis(3,5-difluorophenyl)pyrrole (4.9 g, 0.017 mol) in 6.4% yield (based on 3,5,3′,5′-tetrafluorobenzil). ^{1}H NMR ($CDCl_3$): δ 8.41 (br s, 1H, NH), 6.92 (d, 2H, J = 3.5 Hz, pyrrole-H_α), 6.75 (m, 4H, H_{ortho}), 6.66 (tt, 2H, H_{para}). ^{19}F NMR ($CDCl_3$): δ −112.3 (m, F_{meta}). Mp: 185

(25) Lin, X. Q.; Kadish, K. M. *Anal. Chem.* **1985**, *57*, 1498.
(26) Ohya-Nisiguchi, H. *Bull. Chem. Soc. Jpn.* **1979**, *52*, 2064.
(27) Friedman, M. *J. Org. Chem.* **1965**, *30*, 859.
(28) Medforth, C. J.; Senge, M. O.; Smith, K. M.; Sparks, L. D.; Shelnutt, J. A. *J. Am. Chem. Soc.* **1992**, *114*, 9859.
(29) Williamson, K. L. *Macroscale and Microscale Organic Experiments*; D. C. Heath and Co.: Lexington, MA, 1989; p 534.
(30) Wilcox, C. F. J. *Experimental Organic Chemistry, A Small Scale Approach*; MacMillan Publishing Co.: New York, 1988; p 427.
(31) Selman, S.; Eastham, J. F. *Q. Rev. Chem. Soc.* **1960**, *14*, 221.

°C. FAB HRMS: $[M]^+$ calcd 291.0671, found 291.0675. Anal. Calcd for $C_{16}H_9F_4N$: C 65.98, H 3.11, N 4.81. Found: C 65.75, H 3.03, N 4.78.

Syntheses of Porphyrins. H_2DPP was prepared using the Lindsey type reaction described in our earlier DPP papers.[8,28] The fluorinated dodecaphenylporphyrins were prepared later using the same reaction or the modified Adler−Longo reaction described by Takeda and Sato.[32,33] The modified Adler−Longo reaction was used for the preparation of the dodecaarylporphyrins because it could be done on a larger scale due to the much higher reactant concentrations. However, it was not used to make H_2F_8DPP (meso), H_2F_{20}DPP, H_2F_{28}DPP, or H_2F_{36}DPP because the percentage yields obtained from the modified Adler−Longo reaction are significantly lower than those obtained from the Lindsey reaction.[33]

H_2DPP (4). H_2DPP was prepared as described previously.[28]

FeDPPCl. Iron was inserted into H_2DPP using a standard procedure.[34] H_2DPP (72 mg, 0.059 mmol) was dissolved in a mixture of pyridine (10 mL) and glacial acetic acid (10 mL), and the mixture was heated to 90 °C under an inert atmosphere. Saturated aqueous Fe_2SO_4 (4 mL) was added, and the solution was heated overnight at 100 °C. The mixture was diluted with CH_2Cl_2 (100 mL) and the organic layer washed with 0.02 M HCl (2 × 250 mL). The organic layer was dried over anhydrous Na_2SO_4 and filtered, and the solvent was removed in vacuo to afford crude FeDPPCl. This material was chromatographed on a silica gel column using gradient mixtures of MeOH/CH_2Cl_2 (starting with neat CH_2Cl_2). The combined fractions were washed with 0.02 M HCl (250 mL), dried over anhydrous Na_2SO_4, filtered, and the solvent removed in vacuo. This afforded FeDPPCl (48 mg, 0.037 mmol) in 62% yield. ^{1}H NMR ($CDCl_3$ plus KCN in CD_3OD): δ 9.55 (br, 8H) 7.69 (br, 16H), 7.23 (br t, 8H), 6.81 (br, 16H), 5.81 (br, 4H), 4.02 (br, 8H). FAB HRMS: $[M - Cl]^+$ calcd 1276.4167, found 1276.4186. Visible (CH_2Cl_2): λ_{max} (nm, rel int) 454 (100), 536 (21.3), 576 (16.0).

H_2F_4DPPCl (11). This compound was prepared by adapting a published Adler−Longo type procedure for the preparation of dodecaphenylporphyrins.[32,33] 4-Fluorobenzaldehyde (566 mg, 4.56 mmol) was dissolved in acetic acid (38 mL) and brought to reflux. Subsequently, 3,4-diphenylpyrrole (1.00 g, 4.56 mmol) dissolved in warm acetic acid (22 mL) was added to the refluxing solution. Reflux was continued for 14 h, after which time DDQ (1.04 g, 4.56 mmol) was added to the reaction mixture and reflux was continued for another 60 min. The cooled reaction solution was poured into a mixture of deionized water (300 mL) and saturated aqueous NaCl (300 mL) and neutralized with aqueous NaOH. The aqueous layer was extracted with CH_2Cl_2 (3 × 200 mL), and the combined organic extracts were washed with aqueous 5% NaOH, dried over anhydrous Na_2SO_4, and stripped of solvent in vacuo. The resulting material was chromatographed on a silica gel column using gradient mixtures of MeOH/CH_2Cl_2 (starting with neat CH_2Cl_2 and finishing with neat MeOH). The porphyrin-bearing fractions were crystallized from CH_2Cl_2/cyclohexane, affording H_2F_4DPP (424 mg, 0.327 mmol) in 29% yield. ^{1}H NMR ($CDCl_3$): δ 7.47 (q, 8H, meso-H_{ortho}), 6.39 (t, 8H, meso-H_{meta}), 6.75 (m, 40H, β-phenyl protons). ^{19}F NMR ($CDCl_3$): δ −118.33 (m, meso-F_{para}). FAB HRMS: $[MH]^+$ calcd 1295.4676, found 1295.4680. Visible (1% Et_3N in CH_2Cl_2): λ_{max} (nm) 464 (ϵ 182 000), 560 (8000), 612 (7200); (1% trifluoroacetic acid in CH_2Cl_2) λ_{max} (nm, rel int) 486 (100), 714 (20.9).

FeF_4DPPCl. Iron was inserted into H_2F_4DPP using a standard procedure.[34] $FeCl_2{\cdot}(H_2O)_4$ (30 mg) was added to a refluxing solution of H_2F_4DPP (40 mg, 0.031 mmol) in DMF (6 mL). After 30 min the reaction mixture was allowed to cool to room temperature and 0.1 N HCl was added. A precipitate appeared, which was filtered off and washed with water. The precipitate was chromatographed on grade III alumina with a 50:50 mixture of CH_2Cl_2/cyclohexane. The iron complex fraction was collected, washed with 0.1 M HCl, and evaporated to dryness to afford a residue, which was crystallized from CH_2Cl_2/*n*-hexane. This gave FeF_4DPPCl (18.5 mg, 0.013 mmol) in 43% yield. ^{1}H NMR ($CDCl_3$): δ 12.2 (br, 8H, meso-H_{meta}), 10.2 (br, 16H, β-H_{meta}), 8.2 (v br, 8H, meso-H_{ortho}), 7.1 (v br, 16H, β-H_{ortho}), 5.4 (v br, 8H, meso-H_{ortho}), 4.96 (s, 8H, β-H_{para}), 4.8 (v br, 16H, β-H_{ortho}). ^{19}F NMR ($CDCl_3$): δ −110.3 (m, β-F_{para}). FAB HRMS: $[M - Cl]^+$ calcd 1348.3791, found 1348.3753. Visible (CH_2Cl_2): λ_{max} (nm) 450 (ϵ 90 300), 530 (17 600), 574 (13 000).

H_2F_8DPP (β) (12). Benzaldehyde (208 mg, 1.96 mmol) and 3,4-bis(4-fluorophenyl)pyrrole (500 mg, 1.96 mmol) were treated as described in the preparation of H_2F_4DPP to afford H_2F_8DPP (β) (435 mg, 0.318 mmol) in 65% yield. ^{1}H NMR ($CDCl_3$): δ 7.52 (d, 8H, meso-H_{ortho}), 6.95 (t, 4H, meso-H_{para}), 6.83 (t, 8H, meso-H_{meta}), 6.60 (m, 16H, β-H_{ortho}), 6.38 (t, 16H, β-H_{meta}). ^{19}F NMR ($CDCl_3$): δ −118.9. Mp: >300 °C. MALDI FT-ICR MS: $[MH]^+$ calcd 1367.4, found 1367.4. Visible (CH_2Cl_2): λ_{max} (nm) 464 (ϵ 170 000), 562 (11 000), 612 (10 600), 718 (5200); (1% trifluoroacetic acid in CH_2Cl_2) λ_{max} (nm, rel int) 384 (19.7), 490 (100), 720 (23.2).

FeF_8DPPCl (β). Iron was inserted into H_2F_8DPP (β) (30 mg, 0.022 mmol) using the procedure described for $Fe^{III}F_4$DPPCl and afforded $Fe^{III}F_8$DPPCl (β) (15 mg, 0.010 mmol) in 45% yield. ^{1}H NMR ($CDCl_3$): δ 12.88 (br s, 8H, meso-H_{meta}), 9.51 (br s, 16H, β-H_{meta}), 8.1 (v br, 8H, meso-H_{ortho}), 6.8 (v br, 16H, β-H_{ortho}), 5.5 (v br, 8H, meso-H_{ortho}), 5.45 (br s, 4H, meso-H_{para}), 4.6 (v br, 16H, β-H_{ortho}). ^{19}F NMR ($CDCl_3$): δ −110.7 (β-F_{para}). FAB HRMS: $[M - Cl]^+$ calcd 1420.3414, found 1420.3459. Visible (CH_2Cl_2): λ_{max} (nm) 450 (ϵ 85 200), 534 (17 000), 574 (12 600).

H_2F_8DPP (Meso) (13). H_2F_8DPP (meso) was prepared by adapting a published Lindsey type procedure for the preparation of dodecaphenylporphyrins.[32] A solution containing 3,4-diphenylpyrrole (0.90 g, 4.1 mmol) and 2,6-difluorobenzaldehyde (0.58 g, 4.1 mmol) in CH_2Cl_2 (500 mL) was purged with N_2 for 10 min, after which time $BF_3{\cdot}OEt_2$ (0.25 mL, 2 mmol) was added via syringe. The reaction mixture was shielded from the light and stirred for 24 h. After removal of the solvent in vacuo the solid obtained was refluxed for 2 h with DDQ (0.75 g, 3.3 mmol) in toluene (250 mL). The cooled solution was treated with triethylamine (0.5 mL), and the solvent was removed in vacuo. The resulting material was chromatographed on a silica gel column using gradient mixtures of MeOH/CH_2Cl_2 (starting with neat CH_2Cl_2). The porphyrin-bearing fractions were crystallized from CH_2Cl_2/cyclohexane, giving H_2F_8DPP (meso) (1.1 g, 0.80 mmol) in 81% yield. ^{1}H NMR ($CDCl_3$): δ −1.09 (s, 2H, NH), 6.18 (dd, 8H, J_{HmHp} = 8.5 Hz, J_{HmF} = 7 Hz, meso-H_{meta}), 6.68 (t, 4H, J_{HpHm} = 8.5 Hz, meso-H_{para}), 6.73−6.78 (m, 24H, β-H_{para}, β-H_{meta}), 6.90 (m, 16H, β-H_{ortho}). ^{19}F NMR ($CDCl_3$): δ −108.55 (meso-F_{ortho}). LSIMS: $[MH]^+$ calcd 1367.4, found 1368. Visible (CH_2Cl_2): λ_{max} (nm) 452 (ϵ 215 000), 546 (17 600), 624 (7300), 689 (2400).

FeF_8DPPCl (Meso). Iron was inserted into H_2F_8DPP (meso) (48 mg, 0.035 mmol) using the procedure described for FeF_4DPPCl and afforded FeF_8DPPCl (meso) (30 mg, 0.021 mmol) in 60% yield. ^{1}H NMR ($CDCl_3$): δ 13.0 (br s, 4H, meso-H_{meta}), 12.6 (br s, 4H, meso-H_{meta}), 10.5 (br s, 8H, β-H_{meta}), 10.4 (br s, 8H, β-H_{meta}), 7.7 (v br, 8H, β-H_{ortho}), 6.4 (br s, 4H, meso-H_{para}), 5.1 (v br, 8H, β-H_{ortho}), 5.1(br s, 8H, β-H_{para}). ^{19}F NMR ($CDCl_3$): δ −80.3 (meso-F_{ortho}), −74.8 (meso-F_{ortho}). FAB HRMS: $[M - Cl]^+$ calcd 1420.3414, found 1420.3361. Visible (CH_2Cl_2): λ_{max} (nm) 398 (ϵ 71 600), 436 (93 600).

H_2F_{12}DPP (14). 4-Fluorobenzaldehyde (486 mg, 3.92 mmol) and 3,4-bis(4-fluorophenyl)pyrrole (500 mg, 1.96 mmol) were treated as described in the preparation of H_2F_4DPP, and afforded H_2F_{12}DPP (462 mg, 0.321 mmol) in 33% yield. ^{1}H NMR ($CDCl_3$): δ 7.47 (q, 8H, meso-H_{ortho}), 6.61 (m, 16H, β-H_{ortho}), 6.54 (t, 8H, meso-H_{meta}), 6.47 (t, 16H, β-H_{meta}). ^{19}F NMR ($CDCl_3$): δ −117.9 (β-F_{para}), −116.4 (meso-F_{para}). FAB HRMS: $[MH]^+$ calcd 1439.3922, found 1439.3978. Visible (2% Et_3N in CH_2Cl_2): λ_{max} (nm) 462 (ϵ 182 000), 558 (11 100), 608 (10 000), 712 (5000); (1% trifluoroacetic acid in CH_2Cl_2) λ_{max} (nm, rel int) 488 (100), 716 (27.4).

FeF_{12}DPPCl. Iron was inserted into H_2F_{12}DPP (40 mg, 0.028 mmol) using the procedure described for FeF_4DPPCl and afforded FeF_{12}DPPCl (23 mg, 0.015 mmol) in 54% yield. ^{1}H NMR ($CDCl_3$): δ 12.5 (br, 8H, meso-H_{meta}), 9.7 (br, 16H, β-H_{meta}), 8.0 (v br, 4H, meso-H_{ortho}), 6.9 (v br, 8H, β-H_{ortho}), 5.4 (v br, 4H, meso-H_{ortho}), 4.5 (v br, 8H, β-H_{ortho}). ^{19}F NMR ($CDCl_3$): δ (ppm) −109.3 (β-F_{para}), −107.9 (meso-F_{para}). FAB HRMS: $[M - Cl]^+$ calcd 1492.3037, found 1492.3072. Visible (CH_2Cl_2): λ_{max} (nm) 448 (ϵ 88 700), 534 (17 400), 576 (13 000).

(32) Takeda, J.; Sato, M. *Inorg. Chem.* **1992**, *31*, 2877.
(33) Takeda, J.; Sato, M. *Chem. Pharm. Bull.* **1994**, *42*, 1005.
(34) Fuhrhop, J.-H.; Smith, K. M. In *Porphyrins and Metalloporphyrins*; Smith, K. M., Ed.; Elsevier: Amsterdam, 1975.

H_2F_{20}DPP (15). Pentafluorobenzaldehyde (2.00 g, 10.2 mmol) and 3,4-diphenylpyrrole (2.24 g, 10.2 mmol) were treated as described in the preparation of H_2F_8DPP (meso) to afford H_2F_{20}DPP (1.74 g, 1.1 mmol) in 44% yield. ^{1}H NMR ($CDCl_3$): δ 7.00 (br, 40H, β-H_{phenyl}). ^{19}F NMR ($CDCl_3$): δ −137.5 (d, 8F, F_{ortho}), −156.2 (t, 4F, F_{para}), −166.9 (t, 8F, F_{meta}). MALDI FT-ICR MS: $[M + H]^+$ calcd 1583.3, found 1583.3. Visible (CH_2Cl_2): λ_{max} (nm) 444 (ϵ 164 000), 538 (10 200), 618 (1970); (1% trifluoroacetic acid in CH_2Cl_2) λ_{max} (nm, rel int) 472 (100), 612 (6.54), 666 (5.12).

FeF_{20}DPPCl. Iron was inserted into H_2F_{20}DPP as described elsewhere.[35] Acetonitrile (50 mL) was refluxed for 30 min in oven-dried glassware under an inert atmosphere. $FeCl_2 \cdot 4(H_2O)$ (899 mg, 4.52 mmol) was added to the refluxing mixture, and subsequently H_2F_{20}DPP (143 mg, 0.090 mmol) dissolved in degassed $CHCl_3$ (12 mL) was added to the reaction mixture in a dropwise fashion. Stirring was continued for 10 min after complete addition of the porphyrinic solution. The reaction mixture was poured into CH_2Cl_2 (200 mL) and washed with 0.5 M HCl to convert the product to its FeCl form. The resulting material was chromatographed on a silica gel column using gradient mixtures of MeOH/CH_2Cl_2 (starting with neat CH_2Cl_2). Porphyrin-bearing fractions were washed with 0.5 M HCl, dried over anhydrous Na_2SO_4, and stripped of solvent in vacuo to give FeF_{20}DPPCl (122 mg, 0.073 mmol) in 81% yield. ^{1}H NMR ($CDCl_3$): δ 10.84 (br s, 16H, β-H_{meta}), 7.7 (v br, 8H, β-H_{ortho}), 5.3 (br s, 16H, β-H_{ortho}, β-H_{para}). ^{19}F NMR ($CDCl_3$): δ −98.1, −102.6 (br, 4F each, meso-F_{ortho}), −152.0 (br, 4F, meso-F_{para}), −156.0, −156.1 (br, 4F each, meso-F_{meta}). ^{1}H NMR ($CDCl_3$ + KCN in CD_3OD): δ 7.95 (d, 16H, β-H_{ortho}), 7.35 (t, 16H, β-H_{meta}), 7.20 (t, 8H, β-H_{para}). ^{19}F NMR ($CDCl_3$ + KCN in CD_3OD): δ −160.3 (meso-F_{meta}), −156.3 (meso-F_{para}), −117.2 (meso-F_{ortho}). FAB HRMS: $[M - Cl]^+$ calcd 1636.2283, found 1636.2275. Visible (CH_2Cl_2): λ_{max} (nm, rel int) 400 (76.7), 430 (100).

H_2F_{28}DPP (16). 3,4-Bis(4-fluorophenyl)pyrrole (500 mg, 2.0 mmol) and pentafluorobenzaldehyde (0.24 mL, 2.0 mmol) were treated as described in the preparation of H_2F_8DPP (meso) and afforded H_2F_{28}DPP (150 mg, 0.087 mmol) in 17% yield. ^{1}H NMR ($CDCl_3$): δ −1.51 (br s, 2H, NH), 6.73 (t, 16H, β-H_{meta}), 6.94 (m, 16H, β-H_{ortho}). ^{19}F NMR ($CDCl_3$): δ −136.14 (meso-F_{ortho}), −153.02 (meso-F_{para}), −164.42 (meso-F_{meta}), −113.68 (β-F_{para}). MALDI FT-ICR MS: $[M + H]^+$ calcd 1727.2, found 1727.2. Visible (CH_2Cl_2): λ_{max} (nm) 442 (ϵ 174 000), 538 (17 200), 616 (7100); (1% trifluoroacetic acid in CH_2Cl_2) λ_{max} (nm, rel int) 490 (100), 630 (10.4), 692 (9.7).

FeF_{28}DPPCl. Iron was inserted into H_2F_{28}DPP (52.2 mg, 0.031 mmol) using the procedure described for FeF_{20}DPPCl and afforded FeF_{28}DPPCl (41 mg, 0.023 mmol) in 75% yield. ^{1}H NMR ($CDCl_3$): δ 10.3 (br s, 8H, β-H_{meta}), 10.2 (br s, 8H, β-H_{meta}), 7.7 (very br s, 8H, β-H_{ortho}), 5.2 (very br s, 8H, β-H_{ortho}). ^{19}F NMR ($CDCl_3$): δ −155.4 (meso-F_{meta}), −155.1 (meso-F_{meta}), −149.9 (meso-F_{para}), −106.4 (β-F_{para}), −103.1 (meso-F_{ortho}), −97.9 (meso-F_{ortho}). ^{1}H NMR ($CDCl_3$ + KCN in CD_3OD): δ 8.12 (m, 16H, β-H_{ortho}), 7.16 (t, 16H, β-H_{meta}). ^{19}F NMR ($CDCl_3$ + KCN in CD_3OD): δ −160.0 (meso-F_{meta}), −155.3 (meso-F_{para}), −117.3 (meso-F_{ortho}), −116.3 (β-F_{para}). FAB HRMS: $[M - Cl]^+$ calcd 1780.1529, found 1780.1488. Visible (CH_2Cl_2): λ_{max} (nm) 387 (ϵ 61 400), 430 (94 000).

H_2F_{36}DPP (17). 3,4-Bis(3,5-difluorophenyl)pyrrole (1.00 g, 3.43 mmol) and pentafluorobenzaldehyde (0.673 g, 3.43 mmol) were treated as described in the preparation of H_2F_8DPP (meso). Silica gel column chromatography ($CHCl_3$ eluent) afforded the desired product along with a red contaminant which runs at the same R_f on silica gel and cannot be removed in this fashion. The red contaminant was removed by crystallization from CH_2Cl_2/cyclohexane, which gave pure crystalline H_2F_{36}DPP (175 mg, 0.094 mmol) in 10.9% yield. ^{1}H NMR (acetone-d_6): δ 7.01 (m, 24H). ^{19}F NMR (acetone-d_6): δ −165.7 (meso-F_{meta}), −154.2 (meso-F_{para}), −135.3 (meso-F_{ortho}), −111.4 (β-F_{meta}). FAB HRMS: $[M]^+$ calcd 1870.1583, found 1870.1629. Visible (CH_2Cl_2): λ_{max} (nm) 444 (ϵ 179 000), 540 (15 000), 572 (6690), 620 (5450); (1% trifluoroacetic acid in CH_2Cl_2) λ_{max} (nm, rel int) 480 (100), 616 (6.9), 676 (7.2).

FeF_{36}DPPCl. Iron was inserted into H_2F_{36}DPP (35 mg, 0.019 mmol) using the procedure described for FeF_{20}DPPCl and afforded FeF_{36}DPPCl (29 mg, 0.015 mmol) in 78% yield. ^{1}H NMR ($CDCl_3$): δ 6.5 (br, 16H, β-H_{ortho}), 4.9 (br, 8H, β-H_{para}). ^{19}F NMR ($CDCl_3$): δ −97.1, −103.6 (br, 4F each, meso-F_{ortho}), −107.0, −108.3 (br, 8F each, β-F_{meta}), −147.5 (br, 4F, meso-F_{para}), −153.5, −154.2 (br, 4F each, meso-F_{meta}). FAB HRMS: $[M - Cl]^+$ calcd 1924.078, found 1924.060. Visible (CH_2Cl_2): λ_{max} (nm, rel int) 391 (65.6), 430 (100), 560 (15.6).

Results and Discussion

Synthetic Studies. The series of F_xDPPs presented in this paper are the most recent additions to a growing collection of porphyrins based on the DPP framework.[33,36] At present, it appears that the preparation of F_xDPPs with even more electron-withdrawing fluorophenyl groups is not feasible. For example, we attempted to prepare 3,4-bis(2,6-difluorophenyl)pyrrole in the hope that it could be reacted with pentafluorobenzaldehyde to afford the more electron-withdrawing H_2F_{36}DPP isomer **18**. However, when 2,6,2′,6′-tetrafluorobenzil was used in the same base-catalyzed reaction employed to make 3,4-bis(3,5-difluorophenyl)pyrrole, the only product isolated was methyl 2,6,2′,6′-tetrafluorobenziloate (some methyl benziloate was obtained in the synthesis of 3,4-bis(4-fluorophenyl)pyrrole, and the methyl benziloate was the major product obtained from the synthesis of 3,4-bis(3,5-difluorophenyl)pyrrole). The fact that the methyl benziloate becomes the major product as the fluorination of the benzil is increased is consistent with a report in the literature that fluorination increases the rate of the benzilic acid rearrangement.[37] A second route involving a base-catalyzed condensation was also used in an attempt to prepare 3,4-bis(2,3,4,5,6-pentafluorophenyl)pyrrole, which upon reaction with pentafluorobenzaldehyde might yield the perfluorododecaphenylporphyrin H_2F_{60}DPP (**19**). However, reaction of 1-cyano-1,2-bis(2,3,4,5,6-pentafluorophenyl)ethene with ethyl isocyanoacetate[38] actually yielded 2,4-dicarbethoxy-3-(2,3,4,5,6-pentafluorophenyl)pyrrole as the principal product; a similar reaction has been reported during the attempted preparation of 3,4-dialkylpyrroles using the same methodology.[39]

Given the difficulties encountered in preparing 3,4-diphenylpyrroles with highly fluorinated phenyl rings, as well as the problems inherent in condensing electron-deficient pyrroles with aldehydes,[40] we turned our attention to the recently reported Suzuki coupling reaction of aryl boronic acids with **3** to give dodecaarylporphyrins.[41] The Suzuki coupling reactions worked well with phenylboronic acid, 4-chlorophenylboronic acid, and 3,5-dichlorophenylboronic acid.[22] However, the reactions of 2,6-difluorophenylboronic acid or 2,3,4,5,6-pentafluorophenylboronic acid with **3** did not give the expected products H_2F_{16}DPP (**20**) or H_2F_{40}DPP (**21**). Further investigations of the uses of the Suzuki coupling reaction to prepare novel DPPs will be reported shortly.[22]

Electrochemical Studies. The electrochemistry of iron porphyrins has been studied in a variety of nonaqueous solvents.[42,43] Low valent iron porphyrins are known to react with chlorinated hydrocarbons such as CH_2Cl_2 to give σ-bonded Fe(III) deriva-

(35) Langry, K. C. Ph.D. Thesis, University of California at Davis, 1982.

(36) Guilard, R.; Perie, K.; Barbe, J.-M.; Nurco, D.; Smith, K. M.; Van Caemelbecke, E.; Kadish, K. M. *Inorg. Chem.* **1998**, *37*, 973.
(37) Chamber, R. D.; Clark, M.; Spring, D. J. *J. Chem. Soc., Perkin Trans. 1* **1972**, 2464.
(38) Barton, D. H.; Zard, S. Z. *J. Chem. Soc., Chem. Commun.* **1985**, 1098.
(39) Ono, N.; Maruyama, K. *Bull. Chem. Soc. Jpn.* **1988**, *61*, 4470.
(40) Kaesler, R. W.; LeGoff, E. *J. Org. Chem.* **1982**, *47*, 5246.
(41) Zhou, X.; Tse, M. K.; Wan, T. S.; Chan, K. S. *J. Org. Chem.* **1996**, *61*, 3590.
(42) Kadish, K. M. *Prog. Inorg. Chem.* **1986**, *34*, 435.
(43) Kadish, K. M. In *Iron Porphyrins*; Lever, A. B. P., Gray, H. B., Eds.; Addison-Wesley: Reading, MA, 1983; p 161.

Table 1. Half-Wave Potentials ($E_{1/2}$, V vs SCE) for Oxidation of Chloroiron(III) Porphyrins in CH_2Cl_2, 0.1 M TBAP

porphyrin	first ox.	second ox.	Δ_{ox}
OEP[42,43]	1.08	1.30	0.22
TPP[42,43]	1.14	1.43	0.29
DPP	0.73	1.19	0.46
F_4DPP	0.78	1.16	0.38
F_8DPP (β)	0.82	1.19	0.37
F_{12}DPP	0.84	1.18	0.34
F_8DPP (meso)	1.06	1.41	0.35
F_{20}DPP	1.36	1.64	0.28
F_{28}DPP	1.45	*a*	
F_{36}DPP	1.40[b]	*a*	
$\Delta_{FLUORINATION}$[c]	+0.72	+0.45	

[a] Process occurs at potentials too positive to measure. [b] E_{pa} at a scan rate of 0.1 V/s. [c] Anodic shift for most highly fluorinated derivative versus least fluorinated derivative.

Scheme 1

$$Fe^{III}PCl \overset{-e^-}{\rightleftharpoons} [Fe^{III}PCl]^{+\bullet} \overset{-e^-}{\rightleftharpoons} [Fe^{III}PCl]^{2+}$$

tives,[44] so we used CH_2Cl_2 as a solvent only for oxidation reactions. Benzonitrile or pyridine was employed for the reduction reactions.

Electrooxidation in CH_2Cl_2. Table 1 summarizes the half-wave potentials for the oxidations of each investigated complex along with those for the well-studied FeTPPCl and FeOEPCl under the same experimental conditions. The F_xDPP derivatives with $x = 0-20$ undergo two well-defined one-electron transfer processes while FeF_{28}DPPCl and FeF_{36}DPPCl show only a single oxidation within the anodic potential range of the solvent. The redox reactions are straightforward, and the overall reactions proceed as shown in Scheme 1, where P represents F_xDPP and the final products are formulated as Fe(III) porphyrin π-radical cations and π-dications, respectively.[42,43]

As was earlier reported,[45] FeDPPCl is much easier to oxidize ($E_{1/2} = 0.73$ V) than either FeTPPCl ($E_{1/2} = 1.14$ V) or FeOEPCl ($E_{1/2} = 1.08$ V), something which would not be expected on the basis of the electronic effects of the substituents. The easier oxidation of FeDPPCl is consistent with the fact that the compound adopts a very nonplanar conformation in solution.[1,3,46]

The oxidation potentials of the FeF_xDPPCls show the expected increase with the degree of fluorination of the peripheral phenyl rings, with $\Delta_{FLUORINATION}$ for the first oxidation potential changing by approximately 720 mV within the series (Table 1). However, the $E_{1/2}$ values for oxidation of FeDPPCl, FeF_4DPPCl, FeF_8DPPCl (β), and FeF_{12}DPPCl do not show a simple linear relationship with the number of F groups on the porphyrin macrocycle. This and other data in Table 1 suggest that the electron-withdrawing abilities of the fluoro groups depend, on one hand, on where they are located on the phenyl group (i.e., at the ortho, meso, or para position) and, on the other hand, on where the substituted phenyl groups are located on the porphyrin macrocycle (i.e., at the meso or β positions). Attempts were made to correlate the oxidation potentials seen for the FeF_xDPPCl complexes with empirical measures of the electron-withdrawing ability of the substituents (Hammett σ values), but the analysis was not conclusive, due in part to differences in the reported Hammett σ values for fluorophenyl substituents and in part to the fact that these values were not available for some substituents. A more detailed investigation of the substituent effects in these and other F_x-DPP complexes is in progress and will be reported shortly.[47]

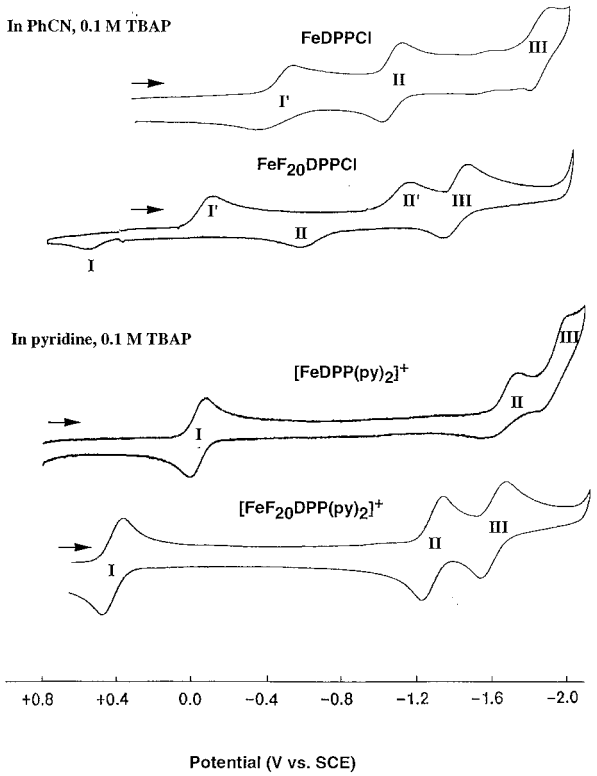

Figure 2. Cyclic voltammograms for the electroreduction of chloroiron(III) porphyrins in benzonitrile/0.1 M TBAP or pyridine/0.1 M TBAP. Scan rate = 0.1 V/s.

Finally, a comparison of the oxidation potentials for FeDPPCl and FeF_{20}DPPCl shows that the potential difference is somewhat greater for the first oxidation (630 mV) than for the second oxidation (450 mV). Indeed, the second oxidation of the FeF_x-DPPCls is virtually unaffected by the addition of 4, 8, or 12 F groups at the para position of the phenyl rings in DPP, F_4DPP, F_8DPP, or F_{12}DPP. This lack of a substituent effect of the F groups on the second oxidation is reflected in the absolute potential separation between the two redox processes of a given compound (Δ_{ox}) which systematically decreases from 0.46 V for FeDPPCl to 0.34 V for FeF_{12}DPPCl (Table 1).

Electroreduction in Benzonitrile. Figure 2 shows the reduction of FeDPPCl and FeF_{20}DPPCl in benzonitrile containing 0.1 M TBAP. Two types of behavior are observed. The first is for FeDPPCl, which undergoes three reversible one-electron reductions at $E_{1/2} = -0.36$, -0.99, and -1.76 V. A different type of behavior is seen for the fluorinated derivatives, where the first two reductions are generally coupled with chemical reactions and show large separations between the cathodic and anodic peak potentials (see Table 2 and Figure 2). The separations between the anodic and cathodic peak potentials, $|E_{pa} - E_{pc}|$, are equal to 0.68 and 0.51 V for the first reduction of the F_{20} and F_{28} derivatives and 0.73 V for the first reduction of FeF_{36}DPPCl.

The irreversible nature of the Fe(III)/Fe(II) process for the FeF_xDPPCl complexes is characterized by current−voltage

(44) Lexa, D.; Mispelter, J.; Saveant, J. M. *J. Am. Chem. Soc.* **1981**, *103*, 6806.
(45) Takeda, J.; Sato, M. *Chem. Lett.* **1995**, 939.
(46) Barkigia, K. M.; Renner, M. W.; Furenlid, L. R.; Medforth, C. J.; Smith, K. M.; Fajer, J. *J. Am. Chem. Soc.* **1993**, *115*, 3627.
(47) Kadish, K. M.; Van Caemelbecke, E.; D'Souza, F.; Lin, M.; Forsyth, T. P.; Medforth, C. J.; Krattinger, B.; Nurco, D. J.; Smith, K. M.; Shelnutt, J. A. Manuscript in preparation.

Table 2. Potentials (V vs SCE) for Reduction of Chloroiron(III) Porphyrins in Benzonitrile Containing 0.1 M TBAP

	first red.			second red.			
porphyrin	E_{pc} (I′)	E_{pa} (I)	Δ^a (V)	E_{pc} (II′)	E_{pa} (II)	Δ^a (V)	third red. $E_{1/2}$ (III)
OEP	−0.54[b]			−1.26[b]			
TPP	−0.29[b]			−1.06[b]			−1.73
DPP	−0.35[b]				−0.99[b]		−1.76
F_4DPP	−0.34	−0.01	0.33	−1.31	−0.90	0.41	−1.66
F_8DPP (β)	−0.33	0.01	0.34	−1.41	−0.87	0.54	−1.63
F_{12}DPP	−0.28	0.04	0.32	−1.24[c]	−0.84	0.40	−1.58
F_8DPP (meso)	−0.27	0.15	0.42	−1.42[d]	−0.91	0.51	−1.67
F_{20}DPP	−0.10	0.58	0.68	−1.14	−0.56	0.58	−1.37
F_{28}DPP	−0.04	0.47	0.51	−1.12	−0.46	0.66	−1.28
F_{36}DPP	+0.12	0.85	0.73	−0.88	−0.30	0.58	−1.10
$\Delta_{FLUORINATION}$[e]	+0.47	+0.86		+0.43	+0.69		+0.66

[a] $\Delta = |E_{pc} - E_{pa}|$. [b] $E_{1/2}$ value. [c] Additional reversible reaction seen at −0.90 V. [d] Additional peak potential at −1.18 V. [e] Anodic shift for most highly fluorinated derivative versus least fluorinated derivative.

Scheme 2

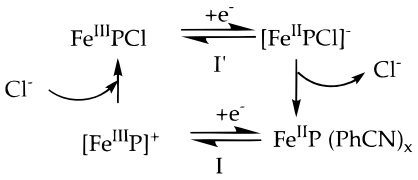

Scheme 3

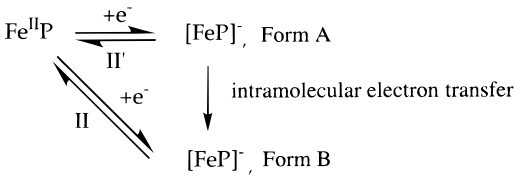

curves similar to those reported for FeTPPCl or FeOEPCl under several experimental conditions.[42,43] The prevailing mechanism for these reductions is shown in Scheme 2, where processes I′ and I correspond to the reduction and reoxidation peaks of the Fe(III)/Fe(II) process as indicated in Figure 2.

The formation of a spectrally detectable Fe(II) porphyrin product containing bound Cl^- after reduction of FeTPPCl (i.e., $[Fe^{II}TPPCl]^-$) has been documented in the literature.[48] The mechanism in Scheme 2 was confirmed by the addition of excess TBACl to solutions of the FeF_xDPPCl complexes, which resulted in a completely reversible first reduction. The iron(II) product generated after loss of Cl^- from $[Fe^{II}PCl]^-$ is designated $Fe^{II}P(PhCN)_x$, as previous studies on porphyrins containing electron-withdrawing groups have shown an increased affinity for axial ligands[19] and one or two benzonitrile molecules may bind to the Fe(II) form of the porphyrin.

The electrochemical data in Table 2 and Figure 2 might at first suggest a similar "box mechanism" involving the slow loss of Cl^- upon the conversion of $[FeF_xDPPCl]^-$ to its doubly reduced form (reaction II′). However, on the basis of electrochemical and spectroscopic data, the "box mechanism" was rejected in favor of the one where forms A and B are assigned as an Fe(II) porphyrin π-anion radical and an Fe(I) porphyrin, respectively (Scheme 3). In this case, the second electron transfer for the fluorinated compounds occurs at the macrocycle (process II′) and the electrogenerated compound is converted to the corresponding iron(I) porphyrin species. This conversion may involve a loss of one or two benzonitrile ligands bound to the iron(II) π-anion radical. A change in the coordination of the metal ion could switch the electron transfer site from the porphyrin ring to the metal ion as has been reported earlier in the case of nickel(II) porphyrins.[49] The ultimate iron(I) species is then reoxidized via process II to give $Fe^{II}P$.

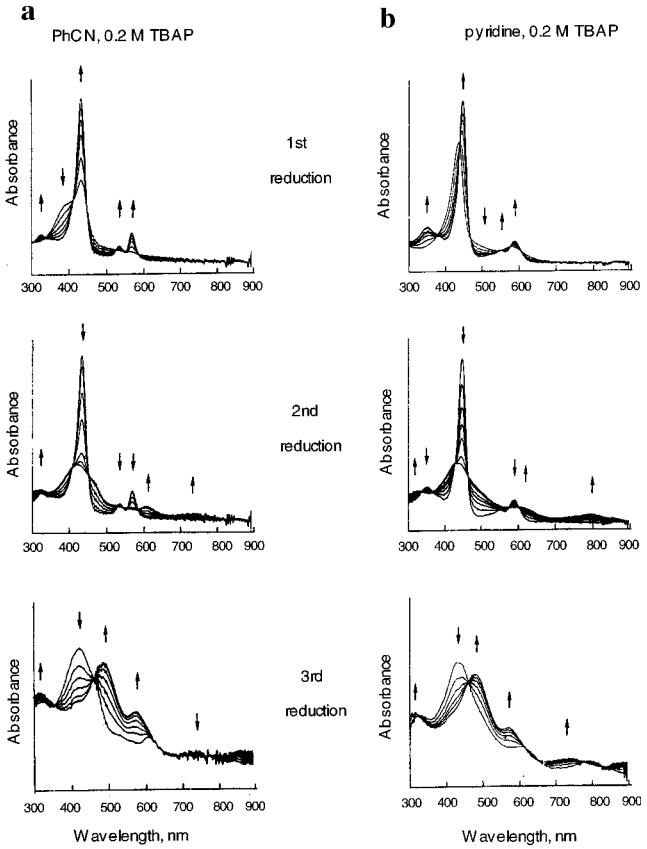

Figure 3. Spectral changes for the first, second, and third one-electron reductions of $FeF_{20}DPPCl$ in (a) benzonitrile/0.2 M TBAP and (b) pyridine/0.2 M TBAP.

Our assignment of form A as an Fe(II) porphyrin π-anion radical for the FeF_xDPPCl compounds is consistent with the much more difficult reduction versus reoxidation (e.g., $E_{pc} = -1.31$ V and $E_{pa} = -0.90$ V for F_4DPP) and the fact that the second reductions of the F_4DPP, F_8DPP, and $F_{12}DPP$ derivatives occur at potentials similar to those for the first macrocycle-centered reduction of MDPP where M = Zn (−1.34 V), Cu (−1.32 V), or Pd (−1.32 V).[45] In addition, the reoxidation peak after the chemical reaction involving doubly reduced FeF_xDPPCl occurs at potentials more positive than those for the metal-centered Fe(I)/Fe(II) reaction of FeDPPCl, consistent with a metal-centered reoxidation whose $E_{1/2}$ has been shifted by the electron-withdrawing F groups.

UV−visible spectroelectrochemical data were obtained for $FeF_{20}DPPCl$ and are consistent with the electrochemical results. The spectral changes upon the first reduction of $FeF_{20}DPPCl$ in benzonitrile are illustrated in Figure 3, and a summary of the spectral data is given in Table 3. The spectral changes during reduction are similar to those reported for other iron(III) porphyrins bearing an anionic axial ligand,[19,50] and the data in

(48) Kadish, K. M.; Rhodes, R. K. *Inorg. Chem.* **1983**, *22*, 1090.

(49) Kadish, K. M.; Franzen, M. M.; Han, B. C.; Araullomcadams, C.; Sazou, D. *J. Am. Chem. Soc.* **1991**, *113*, 512.

(50) Grinstaff, M. W.; Hill, M. G.; Labinger, J. A.; Gray, H. G. *Science* **1994**, *264*, 1311.

Table 3. Absorption Maxima for $FeF_{20}DPPCl$ and Its Electroreduced Products in Benzonitrile and Pyridine Containing 0.2 M TBAP

redox reactn	solvent	λ_{max}, nm			
none	benzonitrile	389	432		
	pyridine	348	441		586
first red.	benzonitrile	327	432	534	568
	pyridine	351	447	551	588
second red.	benzonitrile	319	422	605	738
	pyridine	323	430	609	794
third red.	benzonitrile	311	486	574	
	pyridine	310	475	568	736

Figure 3 are consistent with the generation of either $[Fe^{II}F_{20}DPPCl]^-$ or $Fe^{II}F_{20}DPP$ as a final reduction product after addition of one electron. The current−voltage curves for this electrode reaction are consistent with an EC mechanism where the chemical step, C, involves Cl^- dissociation. Thus, $Fe^{II}F_{20}DPP$ is the expected final porphyrin product after complete electrolysis of $Fe^{III}F_{20}DPPCl$ at −0.5 V. The spectral changes after reduction of $FeF_{20}DPPCl$ by one electron are reversible, and the UV−visible spectrum of the initial Fe(III) porphyrin could be regenerated by controlled-potential oxidation at 0.8 V. This spectrum could also be recovered by switching the potential back to 0.8 V after the *second* one-electron reduction of $FeF_{20}DPPCl$.

The UV−visible data does not unambiguously distinguish between electrogeneration of an Fe(II) porphyrin π-anion radical or an Fe(I) porphyrin in the second one-electron addition. However, because the second reduction is irreversible by cyclic voltammetry at a scan rate of 0.1V/s in benzonitrile (see Figure 2), the porphyrin product detected in solution by thin-layer UV−visible spectroelectrochemistry should be form B (i.e., $[Fe^{I}F_{20}DPP]^-$) on the slower spectroelectrochemistry time scale. Iron(I) porphyrins have been reported to have a split Soret band and broad absorption bands between 700 and 800 nm,[51] and both of these Fe(I) features are present in the UV−visible spectrum generated after complete electrolysis of $Fe^{II}F_{20}DPP$ at −1.4 V.

The initial generation of an Fe(II) porphyrin π-anion radical and the subsequent conversion to an Fe(I) porphyrin as a final product of the two-electron reduction are further confirmed by the ESR spectrum for doubly reduced $FeF_{20}DPPCl$ in benzonitrile (Figure 4a). When the doubly reduced $FeF_{20}DPPCl$ was generated chemically by the reduction of $FeF_{20}DPPCl$ (1.0 mM) with 2 equiv of $Ru(bpy)_3^+$ (2.0 mM) in benzonitrile, the ESR spectrum taken just after the reduction at 77 K in Figure 4a shows both an isotropic signal ($g = 2.003$) and an anisotropic signal characteristic of an axially symmetric spin system ($g_{\|} = 1.955$ and $g_{\perp} = 2.168$). The isotropic signal can be assigned to an Fe(II) porphyrin π-anion radical, while the anisotropic signal is similar to those of $[Fe^{I}TPP]^-$ ($g_{\|} = 1.93$ and $g_{\perp} = 2.28$)[52] and $[Fe^{I}TPPBr_7]^-$ ($g_{\|} = 1.96$ and $g_{\perp} = 2.21$).[51] When the doubly reduced $FeF_{20}DPPCl$ was generated electrochemically, the anisotropic signal was mainly observed with a trace amount of the isotropic signal. Thus, the two-electron reduction of $FeF_{20}DPPCl$ results in the initial formation of the Fe(II) porphyrin π-anion radical, which is then converted to the Fe(I) porphyrin via intramolecular electron transfer. The two-electron reduction of $FeF_{28}DPPCl$ (1.0 mM) with 2 equiv of $Ru(bpy)_3^+$ (2.0 mM) also results in the formation of both the Fe(II) porphyrin π-anion radical ($g = 2.004$) and the Fe(I) porphyrin ($g_{\|} = 1.954$ and $g_{\perp} = 2.158$).

(51) Donohoe, R. J.; Atamian, M.; Bocian, D. F. *J. Am. Chem. Soc.* **1987**, *109*, 5593.
(52) Yamaguchi, K.; Morishima, I. *Inorg. Chem.* **1992**, *31*, 3216.

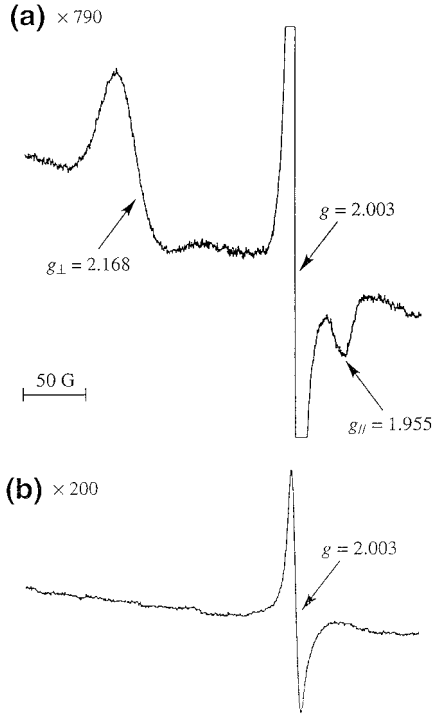

Figure 4. ESR spectra of doubly reduced $FeF_{20}DPPCl$ at 77 K in (a) benzonitrile/0.2 M TBAP and (b) pyridine/0.2 M TBAP. The spectra were generated in situ after chemical reduction of the porphyrin using 2 equiv of $Ru(bpy)_3^+$.

The reduction site for Fe(II) porphyrins had been a major point of controversy in the literature for a number of years prior to the definitive ESR study by Bocian and co-workers[51] which showed that an iron(II) porphyrin π-anion radical or an iron(I) porphyrin could be observed depending upon the substituents on the macrocycle. Porphyrins with the most electron-withdrawing substituents favored reduction at the macrocycle, as the porphyrin e_g orbitals were at lower energy than the metal $d_{x^2-y^2}$ and d_{z^2} orbitals. Alternatively, porphyrins with the least electron-withdrawing substituents underwent reduction at the iron center because the d_{z^2} orbitals were lower in energy than the porphyrin e_g orbitals. A similar explanation can be offered for the DPP and F_xDPP complexes investigated in this study, where reduction of the electron-deficient FeF_xDPPCls also takes place at the macrocycle. More significantly, the FeF_xDPPCl complexes clearly demonstrate the conversion of an Fe(II) porphyrin π-anion radical to an Fe(I) porphyrin via intramolecular electon transfer.

The third reduction of FeF_xDPPCl is spectrally and electrochemically reversible in benzonitrile (see Figures 2 and 3) and is proposed to involve a conversion of the Fe(I) porphyrin to an Fe(I) π-anion radical, thus giving the electron transfer processes shown in Scheme 4 for the overall three-electron reduction of the compounds investigated. Each FeF_xDPPCl derivative has a potential separation of 740−820 mV between $E_{1/2}$ of process III and E_{pa} of process II, which is similar to the 770 mV separation between processes III and II of FeDPPCl where the second reduction involves formation of Fe(I) followed by formation of an Fe(I) π-anion radical at more negative potentials.

The reduction potentials of the FeF_xDPPCl complexes in benzonitrile (Table 2) clearly show the same anodic shifts seen when the compounds were oxidized in CH_2Cl_2 (Table 1). The range of potentials ($\Delta_{FLUORINATION}$) seen for the metal-centered reduction process I′ $[Fe^{III}PCl \rightarrow Fe^{II}PCl]^-$ was 450 mV, versus

Scheme 4

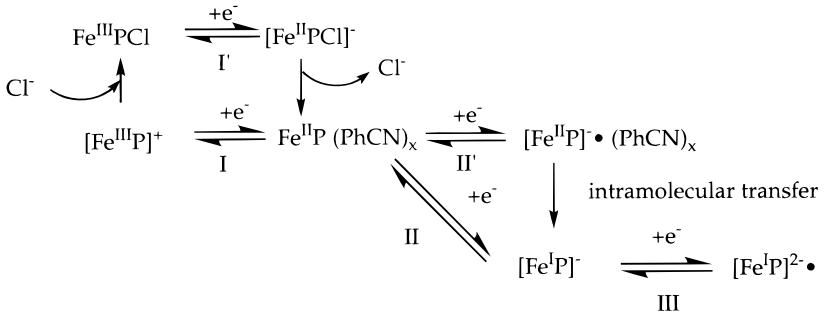

Table 4. Half-Wave Potentials (V vs SCE) for Reduction of Chloroiron(III) Porphyrin Complexes in Pyridine Containing 0.1 M TBAP

porphyrin	first red. process I	second red. process II	third red. process III
OEP[42,43]	−0.02	−1.80	
TPP[42,43]	0.17	−1.45	
DPP	−0.01	−1.58	−1.85
F_4DPP	0.06	−1.50	−1.76
F_8DPP (β)	0.09	−1.48	−1.75
F_{12}DPP	0.07	−1.44	−1.74
F_8DPP (meso)	0.12	−1.49	−1.76
F_{20}DPP	0.45	−1.19	−1.53
F_{28}DPP	0.53	−1.07	−1.44
F_{36}DPP	0.58	−0.88	−1.27
$\Delta_{FLUORINATION}$[a]	0.59	0.70	0.58

[a] Anodic shift for most highly fluorinated derivative versus least fluorinated derivative.

430 mV for the macrocycle-centered second reduction process II′ [$Fe^{II}P \rightarrow Fe^{II}P^-$] and 660 mV for the macrocycle-centered third reduction process III [$Fe^{I}P \rightarrow Fe^{I}P^-$]. $\Delta_{FLUORINATION}$ values for the corresponding reoxidations were larger, with process I giving $\Delta_{FLUORINATION}$ = 860 mV and process II showing $\Delta_{FLUORINATION}$ = 690 mV. These can be compared to a $\Delta_{FLUORINATION}$ value of 720 mV for the first macrocycle-centered oxidation process.

Electroreduction in Pyridine. Figure 2 also illustrates cyclic voltammograms for the reduction of FeDPPCl and FeF_{20}DPPCl in pyridine with 0.1 M TBAP. The potentials for each redox process are summarized in Table 4, which also includes data for FeOEPCl and FeTPPCl. Each FeF_xDPPCl complex undergoes three one-electron transfers, which are labeled as processes I−III. The reversible half-wave potentials shift in a positive direction (easier reduction) with increased degree of fluorination. A 340−570 mV anodic shift in the Fe(III)/Fe(II) process is also observed for each given compound upon going from benzonitrile to pyridine as a solvent, and this can be interpreted in terms of $[FeF_xDPP(py)_2]^+$ formation in the coordinating pyridine solvent. A similar assignment has been made in the case of FeTPPCl.[43,48]

Figure 3 illustrates the UV−visible spectroelectrochemical results for the first, second, and third one-electron reductions of FeF_{20}DPPCl in pyridine. A summary of the spectral data in Figure 3 is also given in Table 3. The wavelengths of maximum absorbance in pyridine differ significantly from values in benzonitrile, as seen in Figure 3 for the case of FeF_{20}DPPCl. The spectrum of the neutral compound in pyridine has a single Soret band at 441 nm and a broad visible band at 586 nm. In contrast, the spectrum in benzonitrile has a Soret band at 432 nm, a shoulder at 389 nm, and no well-defined visible bands between 500 and 800 nm. The singly reduced product of the $[Fe^{III}F_{20}DPP(py)_2]^+$ complex has a 588 nm band in pyridine, and this suggests that the initial porphyrin may actually exist as a mixture of Fe(II) and Fe(III) forms of the porphyrin in pyridine, which is perhaps not unexpected given the extremely positive Fe(III)/Fe(II) reduction potential of 0.45 V.

The spectral changes upon controlled-potential reduction of FeF_{20}DPPCl at 0.2 V in pyridine are similar to those after reduction in benzonitrile (see Figure 3) and indicate that a pure iron(II) form of the compound is electrogenerated in both cases. The spectral changes are reversible, and the UV−vis spectrum of $[Fe^{III}F_{20}DPP(py)_2]^+$ could be fully regenerated upon controlled-potential oxidation at 0.6 V. The iron(II) porphyrin electrogenerated in pyridine has a UV−visible spectrum which differs from that of the electrogenerated iron(II) complex in benzonitrile, consistent with the known binding of pyridine to Fe(II) porphyrins.[43,48]

The Soret and visible bands collapse during the second one-electron reduction of FeF_{20}DPPCl, while the band at 351 nm blue shifts to 323 nm and two new bands emerge at 609 and 794 nm. The data in Figure 3 resemble those obtained during the second reduction of the same compound in benzonitrile. However, closer examination of the data in Table 3 suggests that the doubly reduced product in the two solvents has a different formulation. This would be consistent with the different electrochemical behavior of the FeF_xDPPCl complexes in benzonitrile and pyridine, i.e., the second reduction is reversible in pyridine by both regular and thin-layer cyclic voltammetry. The doubly reduced product in pyridine is proposed to exist as the Fe(II) porphyrin π-anion radical $[Fe^{II}F_{20}DPP(py)_x]^{-\bullet}$ where $x = 1$ or 2. This is confirmed by the ESR spectrum of doubly reduced FeF_{20}DPPCl (1.0 mM) produced by the reduction with 2 equiv of $Ru(bpy)_3^{+}$ (2.0 mM) in pyridine (Figure 4b). In this case, only an isotropic ESR signal due to an Fe(II) porphyrin π-anion radical ($g = 2.003$) is observed. No anisotropic signal due to an Fe(I) porphyrin was seen in pyridine, in contrast to the results obtained in benzonitrile (Figure 4a). A similar isotropic signal ($g = 2.004$) was observed for doubly reduced FeF_{28}DPPCl in pyridine.

$[Fe^{II}F_{20}DPP(py)_x]^{-\bullet}$ is further reduced to an Fe(I) π-anion radical as shown by the fact that the UV−visible spectra of triply reduced FeF_{20}DPPCl are virtually the same in benzonitrile and pyridine (see Figure 3). The overall electroreduction mechanism in pyridine for each investigated FeF_xDPPCl complex is thus that shown in Scheme 5.

The tendency for the FeF_xDPPCls in pyridine to be reduced at the macrocycle but not to undergo electron transfer to the metal site can be interpreted in terms of axial ligation raising the energy of the d_{z^2} orbital and effectively destabilizing the iron(I) porphyrin compared to the iron(II) porphyrin π-anion radical.[51] Finally, it should be noted that the large anodic shifts ($\Delta_{FLUORINATION}$ values) previously seen in the FeF_xDPPCl series for oxidation in CH_2Cl_2 (Table 1) or reduction in benzonitrile (Table 2) are also seen for reduction in pyridine (Table 4). The

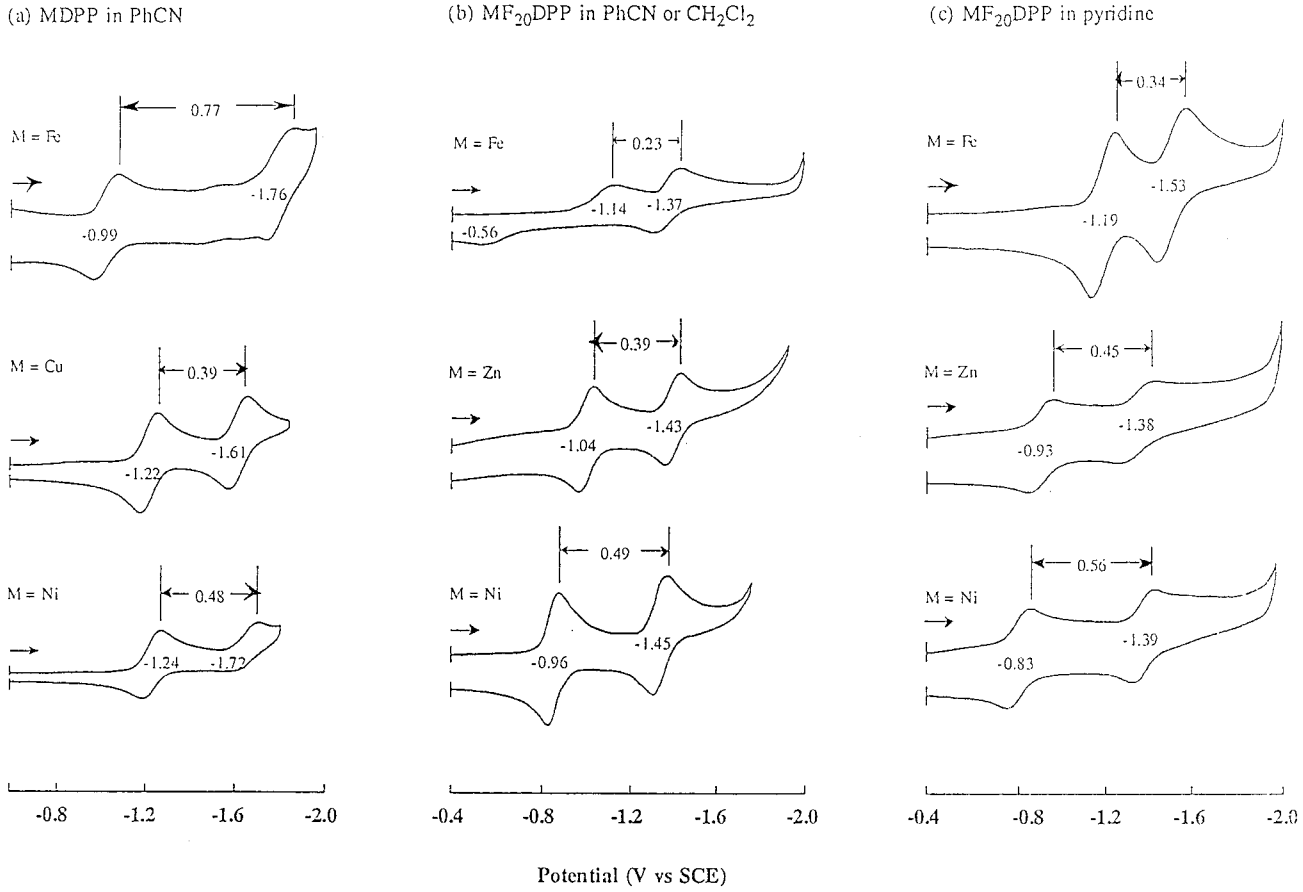

Figure 5. Cyclic voltammograms of (a) MDPPs in benzonitrile/0.1 M TBAP, (b) $MF_{20}DPPs$ in benzonitrile/0.1 M TBAP or CH_2Cl_2/0.1 M TBAP, and (c) $MF_{20}DPPs$ in pyridine/0.1 M TBAP. M = Zn, Fe, Cu, or Ni.

Scheme 5

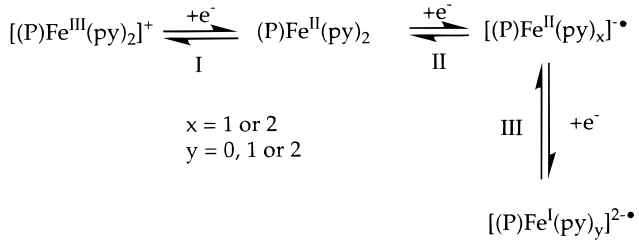

fluorination shifts range from +580 to +700 mV for the three processes observed.

Electroreduction of DPP and F_xDPP Complexes with Other Metals. The electrochemical data obtained for DPP and $MF_{20}DPP$ complexes with other metals (Figure 5 and Table 5) fully support the earlier suggestion that the FeDPPCl and FeF_x-DPPCl complexes are reduced at the metal and at the macrocycle, respectively, in benzonitrile. The macrocycle-centered reductions of CuDPP, NiDPP, and ZnDPP are located at potentials of −1.22 to −1.34 V. In contrast, the potential for the reduction of FeDPPCl in benzonitrile ($E_{1/2}$ = −0.99 V) is lower and is similar to that seen for the first metal-centered reduction of CoDPP ($E_{1/2}$ = −0.97 V in CH_2Cl_2).[45] As expected, the Fe(II) complex also shows a larger absolute potential difference between the two reductions (Δ = 0.77 V) compared to the Zn(II), Cu(II), and Ni(II) DPP complexes (Δ = 0.39−0.49 V). These results are in contrast to those obtained for the corresponding $F_{20}DPP$ derivatives (Table 5), where the reduction potential of the FeDPP complex (E_{pc} = −1.14 V) is similar to those seen for the macrocycle-centered reductions of ZnDPP and NiDPP ($E_{1/2}$ = −1.04 and −0.96 V). Note that the anodic peak potential for reoxidation of $[FeF_{20}DPP]^-$ in benzonitrile is located at a potential almost 500 mV more *positive* than E_{pa} for reoxidation of the other $[MF_{20}DPP]^-$ derivatives, which is consistent with the metal-centered nature of the reoxidation reaction for this species.

Table 5. Half-Wave Potentials (V vs SCE) for Reductions of MDPP and $MF_{20}DPP$ Complexes[a] in Benzonitrile, CH_2Cl_2, or Pyridine with 0.1 M TBAP

porphyrin	metal ion	first red.	second red.	Δ (V)
MDPP (benzonitrile)	$Fe^{III}Cl$	−0.99	−1.76	0.77
	Zn	−1.34[b]	−1.70[b,c]	0.36
	Ni	−1.24	−1.72	0.48
	Cu	−1.22	−1.61	0.39
$MF_{20}DPP$ (benzonitrile or CH_2Cl_2)	$Fe^{III}Cl$	−1.14[c]	−1.37	0.23
	Zn	−1.04	−1.43	0.39
	Ni	−0.96	−1.45	0.49
$MF_{20}DPP$ (pyridine)	$Fe^{III}Cl$	−1.19	−1.53	0.34
	Zn	−0.93	−1.38	0.45
	Ni	−0.83	−1.39	0.56

[a] Details of the syntheses of the other metal complexes are given elsewhere.[53] [b] Reference 45. [c] E_{pc} for irreversible process.

Conclusions

We have synthesized the dodecaphenylporphyrins **4** (DPP) and **11**−**17** (F_xDPPs) with the aim of preparing a series of very nonplanar porphyrins with different electronic properties but similar steric (nonplanarity) effects. Electrochemical investigations of the chloroiron(III) complexes of these porphyrins (abbreviated as FeDPPCl and FeF_xDPPCls) reveal the anodic shifts expected upon fluorination, with the first oxidation potential (FePCl → $[FePCl]^{+\bullet}$) increasing by +720 mV between

FeDPPCl and FeF_{28}DPPCl in CH_2Cl_2/0.1 M TBAP and the porphyrin macrocycle and iron atom also becoming easier to reduce (e.g., $[Fe^{II}P] \rightarrow [Fe^{II}P]^- = +700$ mV for FeDPPCl and FeF_{36}DPPCl in pyridine). Significantly, the electrochemical studies also show that the site of reduction for the iron complexes (i.e., porphyrin ring or central metal) depends upon the solvent and whether the macrocycle is fluorinated. The site of reduction in iron(II) porphyrins had been an area of controversy in the field of porphyrin electrochemistry prior to the definitive ESR studies by Bocian and co-workers[51] which indicated that the iron(II) porphyrin π-anion radicals or iron(I) porphyrins could be obtained depending upon the electron-withdrawing abilities of the substituents. The electrochemical and ESR data presented here show that reduction of (nonfluorinated) Fe^{II}DPP in benzonitrile yields an iron(I) porphyrin whereas reduction of the FeF_xDPP complexes in benzonitrile produces an iron(II) porphyrin π-anion radical. Unusually, in the case of the FeF_xDPP complexes the conversion of the initially produced iron(II) porphyrin π-anion radical to a final iron(I) porphyrin species can also be observed. In contrast to the behavior seen in benzonitrile, all of the complexes yield iron(II) porphyrin π-anion radicals when electroreduced in pyridine.

Additional studies of the F_xDPPs described here are currently in progress. These include attempts to correlate the oxidation and reduction potentials of the F_xDPPs with empirical measures of the electron-withdrawing ability of the substituents, with spectroscopic parameters such as the positions of optical absorption and resonance Raman bands, and with catalytic oxygenation activity in the case of the iron complexes.[47] We are also trying to determine if the effects of electron-withdrawing groups on very nonplanar porphyrins differ from those on nominally planar porphyrins, and to what extent, if any, fluorination changes the structures of DPPs.[22] On the latter point, it should be noted that since we began this project some time ago a number of crystal structures have been reported for DPP and F_xDPP systems.[5,9,53] These investigations have shown that all of the dodecaphenylporphyrins display very nonplanar structures compared to porphyrins without peripheral steric crowding. In addition, they have also revealed a higher degree of structural heterogeneity (i.e., more types of nonplanar distortions) compared to other classes of highly substituted nonplanar porphyrins.[9] Further studies should reveal what influence, if any, such structural heterogeneity has on the chemical, electrochemical, spectroscopic, and dynamic properties of the DPPs, as well as the effect of fluorination on the porphyrin conformation.

Acknowledgment. This work was supported by the Robert A. Welch Foundation (E-680, K.M.K.), by the National Science Foundation (CHE-96-23117) (K.M.S.), and by a Grant-in-Aid for Scientific Research Priority Areas (Nos. 10146232 and 10149230) from the Ministry of Education, Science, Culture and Sports of Japan (S.F.). Sandia is a multiprogram laboratory operated by Sandia Corporation, a Lockheed-Martin company, for the United States Department of Energy under Contract DE-ACO4-94AL85000.

IC9811695

(53) Nurco, D. J. Ph.D. Thesis, University of California at Davis, 1998.